Rev. Roum. Sci. Techn.– Électrotechn. et Énerg.
Vol. **66**, *3*, pp. 181–186, Bucarest, 2021

POWER SUPPLY RESTORATION IN ACTIVE DISTRIBUTION NETWORKS WITH HIGH PHOTOVOLTAIC PENETRATION BASED ON SOFT OPEN POINTS

IRINA PICIOROAGA[1], ANDREI TUDOSE[1], DORIAN SIDEA[1], CONSTANTIN BULAC[1], LUCIAN TOMA[1]

Key words: Active distribution network, Renewable energy sources, Soft open point, Supply restoration, Photovoltaic (PV).

A fundamental concern for the proper functioning of active distribution networks (ADNs) is the continuity of energy supply service. The soft open point (SOP), a device based on power electronics consisting in back-to-back voltage source converters (VSC), represents a flexible solution to improve the performance of ADNs and enhance the service restoration rate in fault conditions. This paper proposes an optimization model based on mixed-integer second-order cone programming to efficiently operate multiple SOPs in order to increase the restoration capability. The performance achieved by SOPs using the proposed model is evaluated for the modified IEEE-33 and IEEE-69 bus systems, considering high photovoltaic (PV) penetration and various load and generation scenarios. The obtained results show improvement in the service restoration rate (by up to 20 %) when SOPs are installed in the ADN.

1. INTRODUCTION

Carbon emissions currently represent a major concern to governments across the world, as global warming effects are threatening the quality of life. The energy sector decarbonization through the mass integration of renewable energy sources (RESs) plays a key role in reducing the greenhouse gas emissions. Beside supporting the low-carbon impact policies, renewable energy sources deployment also stimulates the economic growth [1]. However, due to the rising number of RES-based distributed generation (DG) and the increasing necessity of charging stations for electrical vehicles, new challenges are introduced in the operation of distribution networks. Furthermore, considering other new technologies, such as demand side management and energy storage, the distribution network has to become an active system, which coordinates various devices within the grid to ensure optimal operation conditions, both technically and economically [2, 3]. As a consequence of the high distributed generation penetration, the power flow may shift from unidirectional to a bidirectional mode, leading to the requirement of more complex protection schemes [4]. With massive DG deployment, the distribution network hosting capacity may be reached, generating violations of network operational constraints [5].

Low probability events, such as natural disasters or man-made attacks, represent important threats to the energy supply security. As the extreme events frequency rises, resilience becomes a key component of the active distribution network (ADN) optimal operation [6]. Shortly after a disruptive event, the ADN should possess the capability to restore the supply [7]. Considering the operation near the grid's capacity, in conjunction with the risk of equipment failure, network reinforcements may be required to ensure the resilience of ADNs. Due to environmental constraints and the high investments involved, traditional reinforcement solutions, such as building new electrical lines, present difficulties in terms of implementation [8].

Conventionally, distribution networks are designed in loop configuration, with adjacent feeders connected through tie switches, generally referred to as normally open points (NOPs). To increase the flexibility and reliability of distribution networks, NOPs can be replaced with soft open points (SOPs), which combine the advantages of the radial and meshed structures [9]. Even though current communication infrastructures in the distribution networks do not allow distribution system operators (DSOs) the real-time monitoring and control [10], the future ADNs are expected to have the capability to ensure real-time operation based on intelligent devices, such as SOPs.

The benefits provided by SOPs in ADNs operation were extensively investigated during the past years. Authors of [11] propose a dispatch optimization model for an ADN involving a multi-terminal SOP, that considers the power losses and voltage imbalance reduction. In [12], a model for real-time conservation voltage reduction with SOP and distributed generation dispatch is developed, evaluating the SOP impact on other devices operation, such as the transformers' on-load tap changer systems. The SOP performance in the reconfiguration problem in analyzed in [13] for both ac and dc distribution networks. A coordination methodology for SOPs in an ADN considering the electric vehicles participation in increasing the economic performance is investigated in [14].

In this paper, an optimization model based on mixed-integer second-order cone programming is developed for the supply restoration in active distribution networks in the presence of SOPs. In this regard, two distribution networks with high PV penetration are investigated (IEEE 33 and 69 bus systems), considering several 24 hours loading and generation scenarios. To evaluate the benefits of SOP in extending the restoration rate, comparison studies are conducted with respect to the restored load percentage obtained by applying the conventional reconfiguration process.

2. SUPPLY RESTORATION BASED ON SOFT OPEN POINTS

The soft open point consists of a back-to-back (BtB) connection including two voltage source converters (VSC), as depicted in Fig. 1. Multiple technologies based on power electronics, such as flexible alternating current transmission systems (FACTS) and high-voltage direct current (HVDC) links are already employed in the transmission grid,

[1] "Politehnica" University of Bucharest, Faculty of Energy Engineering, irina.picioroaga@upb.ro

improving its performance and loadability [15], which motivated their implementation in distribution networks as well. Aiming at increasing the DG sources penetration in distribution networks, authors of [16] concluded that SOPs applications (BtB or multi-terminal) ensure better hosting capacity for the network compared to FACTS devices.

SOPs represent a flexible solution for improving distribution networks performance, allowing active and reactive power regulation in both normal and fault conditions. In the power flow control mode, one VSC operates in P-Q mode, establishing the active power flow through the SOP and controlling the reactive power of the converter, while the other VSC operates in V_{DC}-Q mode, providing stable voltage on the dc side and independent reactive power control. During a disturbance occurrence on one feeder of the distribution grid, the SOP isolates the fault and prevents its propagation to the rest of the network. For the supply restoration strategy, the VSC on the faulted side of the grid operates as a voltage source, supplying the faulted area alongside with stable voltage and frequency, while the other VSC operates in V_{DC}-Q mode [17].

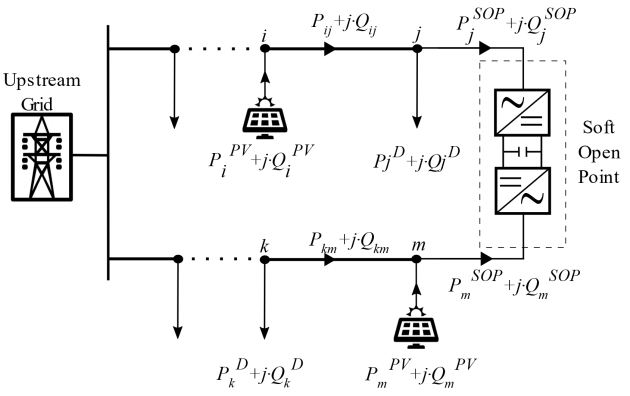

Fig. 1 – Schematic of SOP installation.

To define the SOP operation, the active and reactive power at both VSCs ($P_{i,t}^{SOP}$, $P_{j,t}^{SOP}$, $Q_{i,t}^{SOP}$ and $Q_{j,t}^{SOP}$) are considered decision variables in the model described by eq. (1)−(6) [18]. The power losses that occur during the SOP's operation are modelled based on eq. (2) and eq. (3), where A_i^{SOP} and A_j^{SOP} are the converters loss coefficients. The reactive power output boundaries are established based on $Q_{j,\min}^{SOP}$ and $Q_{j,\max}^{SOP}$ (the minimum and maximum limits), while considering the SOP capacity given by the maximum apparent power at each converter S_i^{SOP} and S_j^{SOP}.

$$P_{i,t}^{SOP} + P_{j,t}^{SOP} + P_{i,t}^{L,SOP} + P_{j,t}^{L,SOP} = 0,\ \forall i,j \in SOP. \quad (1)$$

$$P_{i,t}^{L,SOP} = A_i^{SOP}\sqrt{\left(P_{i,t}^{SOP}\right)^2 + \left(Q_{i,t}^{SOP}\right)^2},\ \forall i \in SOP. \quad (2)$$

$$P_{j,t}^{L,SOP} = A_j^{SOP}\sqrt{\left(P_{j,t}^{SOP}\right)^2 + \left(Q_{j,t}^{SOP}\right)^2},\ \forall j \in SOP. \quad (3)$$

$$Q_{j,\min}^{SOP} \le Q_{j,t}^{SOP} \le Q_{j,\max}^{SOP},\ \ \forall j \in SOP. \quad (4)$$

$$\left(P_{i,t}^{SOP}\right)^2 + \left(Q_{i,t}^{SOP}\right)^2 \le \left(S_i^{SOP}\right)^2,\ \ \forall i \in SOP. \quad (5)$$

$$\left(P_{j,t}^{SOP}\right)^2 + \left(Q_{j,t}^{SOP}\right)^2 \le \left(S_j^{SOP}\right)^2,\ \ \forall j \in SOP. \quad (6)$$

3. SUPPLY RESTORATION METHODOLOGY

In this section, the load recovery maximization methodology based on the optimal coordination of the multiple SOPs is presented. A mixed-integer second-order cone programming (SOCP) model is developed in this regard, where the integer character of the variables refers to the branch and loads status (connected/disconnected).

3.1. OBJECTIVE FUNCTION

Given the SOPs' capability to provide reactive power compensation, thereby contributing to the power losses reduction, a second goal is considered, additionally to the load restoration goal. Therefore, a linear weighted approach is used in (7), aiming at both the service restoration maximization and the total power losses minimization.

$$\begin{aligned} &\min\ F = \alpha_1 \cdot F_{SR} + \alpha_2 \cdot F_{Losses}. \\ &F_{SR} = \sum_{t\in T}\sum_{j\in N}(1-\sigma_{j,t})\cdot w_j \cdot P_{j,t}^{D}. \\ &F_{Losses} = \sum_{t\in T}\left(\sum_{ij\in L}\left(r_{ij}\cdot I_{ij,t}^2\right) + \sum_{i\in SOP} P_i^{L,SOP}\right). \end{aligned} \quad (7)$$

where α_1 and α_2 are the weight coefficients for the two objectives. Function F_{SR} defines the total restored load, where $\sigma_{j,t}$ is a binary variable that models the status of the load j (supplied or unsupplied) during time interval t, while a supply priority is associated to each load j using w_j. Three categories of priority are considered in this study, randomly associated to the buses. $P_{j,t}^{D}$ represents the active power demand at bus j during time interval t. As previously mentioned, a second objective is considered in the proposed model, namely the total active power losses, computed using function F_{Losses}. Here, r_{ij} and $I_{ij,t}$ are the resistance of the line delimited by buses i and j, and the current crossing it, respectively, while $P_i^{L,SOP}$ denotes the active power losses in the SOP's converters. In the previous formulas, the following sets have been used: N - the set of load buses, L - the set of branches, SOP - the set of connection buses for the SOPs converters, while T denotes the analysis time horizon. The restoration rate expansion based on the optimal coordination of the multiple SOPs must be achieved while meeting the operational constraints of SOP and the ADN, as well.

3.2. POWER FLOW CONSTRAINTS

The power flow calculation in the distribution network is performed based on the DistFlow branch model equations proposed in [19]. Eq. (8) and (9) define the power balance at each bus j during time frame t, the voltage drop is computed using (10), while the branch current is determined based on (11).

$$\sum_{jk\in L} P_{jk,t} - \sum_{ij\in L}(P_{ij,t} - r_{ij}I_{ij,t}^2) = P_{j,t}^{PV} + P_{j,t}^{SOP} - \sigma_{j,t}P_{j,t}^{D}. \quad (8)$$

$$\sum_{jk\in L} Q_{jk,t} - \sum_{ij\in L}(Q_{ij,t} - x_{ij}I_{ij,t}^2) = Q_{j,t}^{PV} + Q_{j,t}^{SOP} - \sigma_{j,t}Q_{j,t}^{D}. \quad (9)$$

$$(V_{i,t}^2 - V_{j,t}^2) - 2\left(r_{ij}P_{ij,t} + x_{ij}Q_{ij,t}\right) + (r_{ij}^2 + x_{ij}^2)\cdot I_{ij,t}^2 = 0. \quad (10)$$

$$I_{ij,t}^2 \cdot V_{i,t}^2 \geq P_{ij,t}^2 + Q_{ij,t}^2, \forall ij \in L., \quad (11)$$

where $P_{ij,t}$ and $Q_{ij,t}$ are the active and reactive power flows between buses i and j during time interval t, $P_{j,t}^{PV}$ and $Q_{j,t}^{PV}$ are the active and reactive power of the PV generation unit connected at bus j during time interval t, while $V_{i,t}$ denotes the voltage at bus i.

3.3. SYSTEM OPERATIONAL CONSTRAINTS

For the proper operation of the ADN, the nodal voltages ($V_{j,t}$) and the branch currents must satisfy the limits set by the following constraints:

$$V_{j,\min}^2 \leq V_{j,t}^2 \leq V_{j,\max}^2, \ \forall j \in N. \quad (12)$$

$$0 \leq I_{ij,t}^2 \leq I_{ij,\max}^2, \ \forall ij \in L. \quad (13)$$

The output of the distributed renewable sources installed in the network is limited considering the operational capacity and reactive power boundaries, based on (14) and (15). Here, PV denotes the set of installation buses for the photovoltaics generation units.

$$\left(P_{j,t}^{PV}\right)^2 + \left(Q_{j,t}^{PV}\right)^2 \leq \left(S_j^{PV}\right)^2, \ \forall j \in PV. \quad (14)$$

$$Q_{j,\min}^{PV} \leq Q_{j,t}^{PV} \leq Q_{j,\max}^{PV}, \quad \forall j \in PV. \quad (15)$$

Radiality constraints are formulated based on the methodology presented in [20]. The new radial configuration is calculated immediately after the fault occurrence that led to the power outage and remains the same throughout the rest of the study timeframe.

4. **CASE STUDY**

The performance of the proposed model is tested based on two distribution systems, namely the IEEE 33-bus system and IEEE 69-bus system. For both networks, multiple load and generation scenarios are analyzed in order to verify the SOP benefits in expanding the supply restoration rate.

4.1. IEEE 33−BUS SYSTEM

The first analyzed system is a modified IEEE 33−bus active distribution network, which detailed parameters regarding the maximum bus loads and the lines are specified in [21]. To model the high penetration of renewable sources, six PV generation units have been inserted in the system, as depicted in Fig. 2.

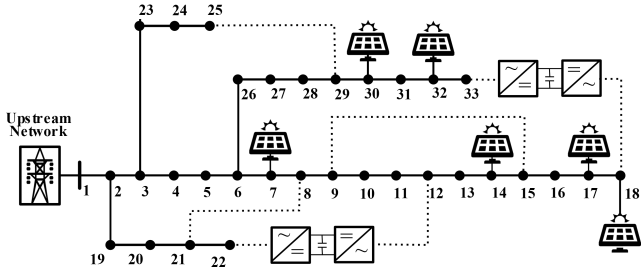

Fig. 2 – The modified IEEE 33−bus system.

Figure 3 illustrates the three load categories (i.e. residential, commercial and industrial) typical to distribution systems and their consumption profiles considered during the simulations, randomly associated to the buses. For each bus, the voltage must be confined within the [0.95, 1.05] p.u. range. The four PV generation units installed at buses 7, 14, 30 and 32, present a rated capacity of 250 kVA, while PV installations connected at buses 17 and 18 have the rated capacity of 150 kVA. For all cases, the power factor is set from 0.95 lagging to 0.95 leading. Figure 4 depicts the generation forecast with hourly resolution for the six sources.

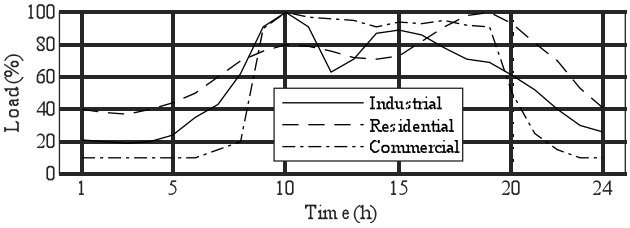

Fig. 3 – The load profiles.

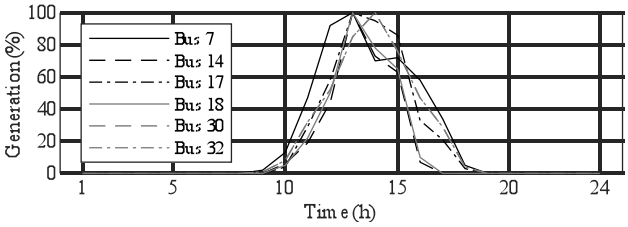

Fig. 4 – The PV generation forecast.

Two SOPs are installed between buses 12 and 22, and between buses 18 and 33, respectively, as depicted in Fig. 2. A maximum capacity of 1000 kVA is considered for each converter. The other parameters of SOP, extracted from [22], include the reactive power range of [−600, 600] kvar, and the active power losses percentage of 2 %.

The restoration analysis conducted in this study focuses on the 24 hours operation of the distribution grid with one-hour time step, while considering a permanent fault occurring on branch 2-3, during the first time interval.

A. Restoration without SOP

The initial IEEE 33−bus system configuration comprises 37 branches, among which 5 normally opened tie switches assure the network radiality. The possibility to alters the feeder topological structure of the distribution network based on the presence of tie switches allows the supply restoration through the reconfiguration procedure. In this case, following the modelled fault, the restoration strategy selects to connect lines 8−21, 12−22, 18−33 and 25−29. Considering the network operation constraints, lines 8−9, 9−15, 24−25 and 28−29 are disconnected to maintain radial topology.

B. Restoration with SOP

As maximizing the load restoration is the main objective, the two weight coefficients in (7) are considered as follows: $\alpha_1 = 0.8$ and $\alpha_2 = 0.2$. The modified configuration of the active distribution network includes two SOPs, along with 3 traditional tie switches. To achieve radiality, lines 6−26, 10−11, 14−15 and 24−25 are disconnected, while lines 8−21, 9−15 and 25−29 are connected.

Given the SOP ability of controlling the converters' reactive power setpoint, the voltage regulation capability is further assessed. In this regard, Fig. 5 depicts the converters reactive power output variation over the 24 hours timeframe. As it can be observed, during the day (08^{00}–21^{00}), the reactive power injection generally increases

to overcome the higher voltage drops occurring in the distribution network due to the peak load hours.

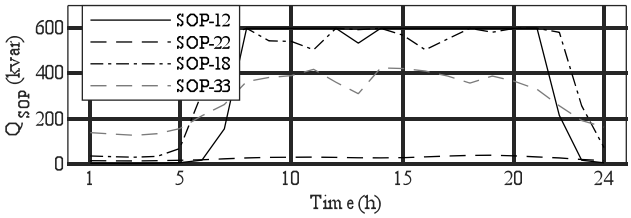

Fig. 5 – Reactive power injection by SOP (IEEE−33).

C. Comparison study – Restoration with and without SOP

For a better exposure of the SOP integration benefits, a comparison study is conducted in this subsection, considering the two supply restorations strategies previously presented above (with and without SOP). The results in terms of load recovery rate for the two schemes in normal loading conditions of the network are presented in Fig. 6. As the SOPs installation facilitates the power transfer between the network feeders, an increase in the restored load percentage can be observed compared to the first restoration scheme, resuming only to the reconfiguration process. However, due to the limited transmission capacity of the rest of lines, a rate of 100 % restoration cannot be achieved during the peak load hours.

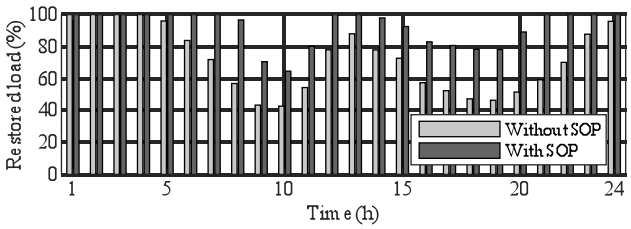

Fig. 6 – Load restoration rate with and without SOP (IEEE−33).

The performance of SOP integration is evaluated by means of voltage level as well. Figure 7 depicts the boxplot representation of the bus voltages for each hour. Major improvements can be observed for SOPs installing, as the hourly minimum and maximum values surpass the no-SOP corresponding value, regardless the loading conditions (peak or off-peak hours). Due to the reactive power injection of SOPs' converters, the maximum voltage for SOP installation is 1.044 p.u. (achieved during the interval 10^{00}–11^{00}), while the maximum voltage obtained without SOP is 1 p.u. (the voltage at the reference bus).

The expansion of supply restoration rate is further assessed considering multiple load and generation scenarios (light, normal and heavy load/generation). Based on the results centralized in Table 1, an improvement can be noticed for all scenarios when SOPs are installed, with increases in power restoration compared with the no-SOP scheme between 9.25 % and 21 %.

Table 1

Supply restoration rate for multiple scenarios (IEEE−33)

	Without SOP			With SOP		
	Light load (60%)	**Normal load (100%)**	**Heavy load (140%)**	**Light load (60%)**	**Normal load (100%)**	**Heavy load (140%)**
PV (60%)	88.39	70.03	56.23	100	90.97	76.04
PV (100%)	89.71	72.23	58.31	100	92.14	78.34
PV (140%)	90.8	73.93	59.85	100	92.57	79.22

The average voltage values for the analyzed scenarios are presented in Table 2. An enhancement in voltage variations can be noted due to the SOP installation, starting from 0.7 % to 2.3 % increase compared to the no−SOP restoration strategy.

Table 2

Average voltage values for multiple scenarios (IEEE−33)

	Without SOP			With SOP		
	Light load (60%)	**Normal load (100%)**	**Heavy load (140%)**	**Light load (60%)**	**Normal load (100%)**	**Heavy load (140%)**
PV (60%)	0.9698	0.963	0.9615	0.9773	0.9808	0.9828
PV (100%)	0.9711	0.9638	0.961	0.9782	0.9793	0.9786
PV (140%)	0.9723	0.9647	0.9612	0.9796	0.9871	0.9807

4.2. IEEE 69−BUS SYSTEM

The second test network analyzed is the IEEE 69−bus system, which parameters can be found in [21]. The base configuration of the network consists of 68 sectionalized lines and 5 normally opened tie switches.

To model high penetration of renewable energy sources in the distribution network, seven PV generation units are installed at buses 8, 12, 21, 49, 50, 61 and 64, each with a rated capacity of 250 kVA. All generation units are set to operate with a power factor from 0.95 lagging to 0.95 leading.

As in the previous study, a 24 hours analysis with one hour time step is performed on the active distribution network, supposing that a permanent three-phase fault occurs on branch 3−4 during the first time interval. Once again, the multiple SOPs coordination advantages in improving the energy supply restoration are verified and compared to the recovery rate resulted by resuming to the network reconfiguration.

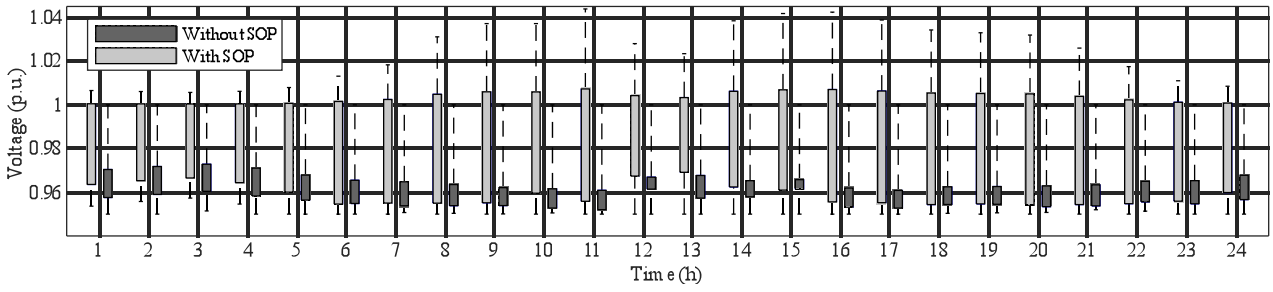

Fig. 7 – Boxplot representation of bus voltages in normal loading and generation conditions (IEEE-33).

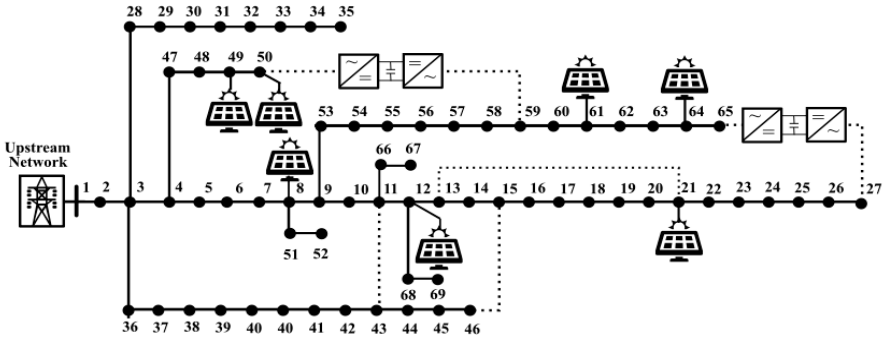

Fig. 8 – The modified IEEE 69−bus system.

A. Restoration without SOP

Firstly, the total unsupplied load is minimized based on the traditional reconfiguration procedure. In this regard, lines 11−43, 13−21, 15−46 27−65 and 50−59 are connected, simultaneously with disconnection of lines 11−12, 13−14, 49−50 and 62−63, to assert the radiality of the network topology.

B. Restoration with SOP

Considering same values for the two weight coefficients (α_1=0.8 and α_2=0.2), the results for the supply restoration in the modified IEEE 69−bus systems are further presented. Two SOPs were installed in the network, connecting buses 27−65 and 50−59, each with the capacity of 800 kVA, reactive power limits in the [−400, 400] kvar range, and the loss coefficients of 2 %, along with 3 traditional tie switches (Fig. 8). To meet the topological constraints, lines 11−43, 13−21, 15−46 27−65 and 50−59 are connected, while lines 11−12, 16−17, 22−23 and 49−50 are disconnected.

Once again, the SOP capability to participate in voltage regulation based on the rapid adjustment in reactive power output is analyzed for normal load and generation conditions. As depicted in Fig. 9, the converters placed at buses 27 and 59 are operating at maximum reactive power capacity most of the day to minimize the power losses during the higher demand hours.

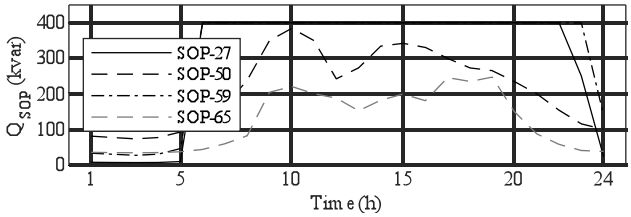

Fig. 9 – Reactive power injection by SOP (IEEE−69).

C. Comparison study – Restoration with and without SOP

Similar to the previous study, the restoration capability of the SOP−involving strategy is compared to the no−SOP strategy. As it can be observed in Fig. 10, for normal load and generation conditions, both strategies restore 100 % of the load during off-peak hours. During peak load hours however, the SOP strategy improve the restoration rate up to 15 %.

The two supply restoration methodologies are once again applied for multiple load and generation scenarios, as summarized in Table 3. In the light load scenario, both strategies achieve 100% restoration rate, while for the normal and heavy load scenarios the SOP installation leads to supply reestablishment expansion by up to 10 %.

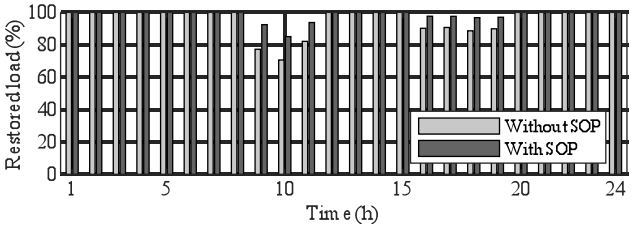

Fig. 10 – Load restoration rate with and without SOP (IEEE−69).

Table 3

Supply restoration rate for multiple scenarios (IEEE−69)

	Without SOP			With SOP		
	Light load (60%)	**Normal load (100%)**	**Heavy load (140%)**	**Light load (60%)**	**Normal load (100%)**	**Heavy load (140%)**
PV (60%)	100	94.38	81.16	100	95.8	88.15
PV (100%)	100	95.4	79.77	100	98.35	89.52
PV (140%)	100	96.01	84.17	100	98.9	91.99

To assess the voltage profile improvement, Fig. 11 presents the boxplots of bus voltages for each hour of the analyzed day for the normal load and generation scenario. As a result of the reactive power compensation provided by SOPs, the voltage profiles are improved compared to the no-SOP scheme, the hourly minimum and maximum reaching superior values in most cases. An average voltage

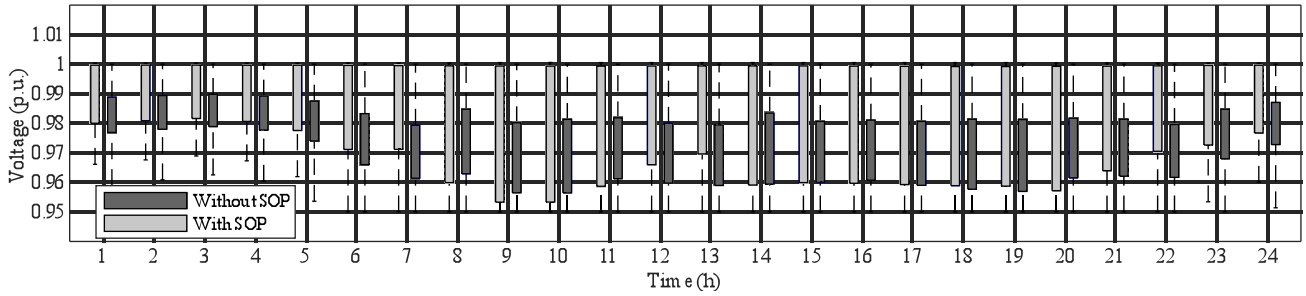

Fig. 11 – Boxplot representation of bus voltages in normal loading and generation conditions (IEEE−69).

enhancement of 0.5 % can be observed in Table 4 in normal conditions. In the heavy load and normal PV scenario, an increase of 1.2 % in the voltage level can be noticed when SOPs are employed.

Table 4

Average voltage values for multiple scenarios (IEEE−69)

	Without SOP			With SOP		
	Light load (60%)	**Normal load (100%)**	**Heavy load (140%)**	**Light load (60%)**	**Normal load (100%)**	**Heavy load (140%)**
PV (60%)	0.9811	0.9754	0.9735	0.9842	0.9799	0.9771
PV (100%)	0.9823	0.9752	0.972	0.9868	0.98	0.9838
PV (140%)	0.9836	0.9764	0.9738	0.9887	0.9797	0.9774

5. **CONCLUSIONS**

The supply service continuity represents a major concern for the active distribution networks operation. In this paper, the capability of soft open points to increase the service restoration rate in active distribution networks with high penetration of renewable energy sources is investigated. In this regard, a mixed−integer second−order cone programming model is proposed to minimize the total unsupplied load based on the optimal operation of SOPs. The study was performed on the IEEE 33−bus and IEEE−69 bus systems modified to employ multiple PV generation units, considering a 24 hours timeframe analysis. To emphasize the SOP integration benefits, several comparison studies have been conducted for various load and generation scenarios. With respect to the conventional restoration strategy resuming to the distribution network reconfiguration, the SOP−based scheme obtained a total restored load increase by up to 20 %. Given the SOP flexibility in reactive power setpoint, the voltage profiles improvement has also been explored, the results reflecting an enhancement by up to 2.3 %.

Received on July 21, 2021

REFERENCES

1. N.E. Koltsaklis, A.S. Dagoumas, G. Seritan, R. Porumb, *Energy transition in the South East Europe: The case of the Romanian power system*, Energy Reports, **6**, pp. 2376–2393 (2020).
2. H. Kiani, K. Hesami, A. Azarhooshang, S. Pirouzi, S. Safaee, *Adaptive robust operation of the active distribution network including renewable and flexible sources*, Sustainable Energy, Grids and Networks, **26**, pp. 100476 (2021).
3. M. Gavrilaş, B. C. Neagu, R.D. Pentiuc, E. Hopulele, *Overview on Distributed Generation Integration in Distribution Systems*, 2018 International Conference and Exposition on Electrical and Power Engineering (EPE), Iasi, Romania, 18-19 Oct. 2018.
4. S E. Razavi, E. Rahimi, M.S. Javadi, A.E. Nezhad, M. Lotfi, M. Shafie-Khah, J. Catalão, *Impact of distributed generation on protection and voltage regulation of distribution systems: A review*, Renewable and Sustainable Energy Reviews, **105**, pp. 157–167 (2019).
5. S.M. Ismael, H.E. Shady, A. Aleem, A.Y. Abdelaziz, A.F. Zobaa, *State-of-the-art of Hosting Capacity in Modern Power Systems with Distributed Generation*, Renewable Energy, **130**, pp. 1002–1020 (2019).
6. I.I. Picioroaga, A.M. Tudose, D.O. Sidea, C. Bulac, L. Toma, *Application of Soft Open Points for Increasing the Supply Restoration in Active Distribution Networks*, 12th International Symposium on Advanced Topics in Electrical Engineering (ATEE), Bucharest, Romania, 25-27 March 2021.
7. D.K. Mishra, M.J. Ghadi, A. Azizivahed, L. Li, J. Zhang, *A review on resilience studies in active distribution systems*, Renewable and Sustainable Energy Reviews, **135**, pp. 110201 (2021).
8. G. Celli, F. Pilo, G.G. Soma, R. Cicoria, G. Mauri, E. Fasciolo, G. Fogliata, *A comparison of distribution network planning solutions: Traditional reinforcement versus integration of distributed energy storage*, 2013 IEEE Grenoble Conference, Grenoble, France, 16-20 June 2013.
9. J. Bloemink, T. Green, *Increasing distributed generation penetration using soft normally-open points*, IEEE PES General Meeting, Minneapolis, MN, USA, 25-29 July 2010.
10. W. Murray, M. Adonis, A. Raji, *Voltage control in future electrical distribution networks*, Renewable and Sustainable Energy Reviews, **146**, pp. 111100 (2021).
11. F. Sun, J. Ma, M. Yu, W. Wei, *Optimized Two-Time Scale Robust Dispatching Method for the Multi-Terminal Soft Open Point in Unbalanced Active Distribution Networks*, IEEE Transactions on Sustainable Energy, **12**, pp. 587–598 (2021).
12. V.B. Pamshetti, S. Singh, A.K. Thakur, S. P. Singh, *Multistage Coordination Volt/VAR Control with CVR in Active Distribution Network in Presence of Inverter-Based DG Units and Soft Open Points*, IEEE Transactions on Industry Applications, **57**, pp. 2035–2047 (2021).
13. M. Khan, A. Wadood, M. Abid, T. Khurshaid, S. Rhee, *Minimization of Network Power Losses in the AC-DC Hybrid Distribution Network through Network Reconfiguration Using Soft Open Point*, Electronics, **10**, pp. 326 (2021).
14. X. Yang, C. Xu, Y. Zhang, W. Yao, J. Wen, S.-J. Cheng, *Real-Time Coordinated Scheduling for ADNs with Soft Open Points and Charging Stations*, IEEE Transactions on Power Systems, early access (2021).
15. M. Ataeizadeh, A. Kargar, S. Abazari, *Optimal location of flexible alternating current transmission systems devices to achieve multiple goals in power systems*, Rev. Roum. des Sci. Techn.–Électrotechn. et Energ., **65**, pp. 27–34 (2020).
16. J.M. Green, T.C. Bloemink, *Benefits of Distribution-Level Power Electronics for Supporting Distributed Generation Growth*, IEEE Transactions on Power Delivery, **28**, pp. 911–919 (2013).
17. W. Cao, J. Wu, N. Jenkins, C. Wang, T. Green, *Operating principle of Soft Open Points for electrical distribution network operation*, Applied Energy, **164**, pp. 245–257 (2016).
18. H. Ji, C. Wang, P. Li, J. Zhao, G. Song, F. Ding, J. Wu, *An enhanced SOCP-based method for feeder load balancing using the multi-terminal soft open point in active distribution networks*, Applied Energy, **208**, pp. 986–995 (2017).
19. M.E. Baran, F.F. Wu, *Network reconfiguration in distribution systems for loss reduction and load balancing*, IEEE Transactions on Power Delivery, **4**, pp. 1401–1407 (1989).
20. R.A. Jabr, R. Singh, B.C. Pal, *Minimum Loss Network Reconfiguration Using Mixed-Integer Convex Programming*, IEEE Transactions on Power Systems, **27**, pp. 1106–1115 (2012).
21. M.Q. Duong, T.D. Pham, T. T. Nguyen, A. T. Doan, H. V. Tran, *Determination of Optimal Location and Sizing of Solar Photovoltaic Distribution Generation Units in Radial Distribution Systems*, Energies, **12**, pp. 174 (2019).
22. H. Ji, C. Wang, P. Li, F. Ding, J. Wu, *Robust Operation of Soft Open Points in Active Distribution Networks with High Penetration of Photovoltaic Integration*, IEEE Transactions on Sustainable Energy, **10**, pp. 280–289 (2019).